Ultralow threshold green lasing and optical bistability in ZBNA ($ZrF_4-BaF_2-NaF-AlF_3$) microspheres

Yuqiang Wu (邬宇强),[1,2] Jonathan M. Ward,[2,3,a)] and Síle Nic Chormaic[1,2,b)]
[1]*Physics Department, University College Cork, Cork, Ireland*
[2]*Photonics Centre, Tyndall National Institute, Lee Maltings, Cork, Ireland*
[3]*Department of Applied Physics and Instrumentation, Cork Institute of Technology, Bishopstown, Cork, Ireland*

(Received 21 July 2009; accepted 1 December 2009; published online 1 February 2010)

Upconversion lasing and fluorescence from active microspheres fabricated from a novel fluorozirconate, Er^{3+} doped glass, ZBNA ($ZrF_4-BaF_2-NaF-AlF_3$), when pumped at 978 nm via a tapered optical fiber is demonstrated. An ultralow, green lasing threshold of ~3 μW for 550 nm emissions is measured. This is one order of magnitude lower than that previously reported for ZBLAN ($ZrF_4-BaF_2-LaF_3-AlF_3-NaF$) microspheres. Optical bistability effects in ZBNA microspheres are reported and the bistable mechanism is discussed and attributed to shifts of the whispering gallery modes due to thermal expansion of the sphere, where heating is achieved by optical pumping around 978 nm. The effect of the bistability on the upconversion lasing is examined and we report multiple bistability loops within the microspheres. © *2010 American Institute of Physics*.
[doi:10.1063/1.3277024]

I. INTRODUCTION

The first demonstration of green upconversion lasing from Er^{3+} (erbium) doped fluorozirconate fiber was reported by Whitley *et al.*[1] Er^{3+} is a triply ionized rare earth ion which acts as gain medium at 1550 nm when pumped at around 978 nm and provides frequency upconversions due to excited state absorption. The first observation of upconversion lasing in rare earth doped glass microspheres was reported by Fujiwara and Sasaki[2] when blue and red lasing of a Tm^{3+} doped fluorozirconate glass microsphere was demonstrated. Subsequently, a green upconversion microsphere laser made of Er^{3+} doped ZBLAN ($ZrF_4-BaF_2-LaF_3-AlF_3-NaF$), with a very low lasing threshold of 30 μW pumped at 801 nm, was demonstrated.[3] More recently, an on-chip green silica upconversion microtoroid laser pumped at 1458 nm and with a lasing threshold of 690 μW has been demonstrated.[4]

The first description of a fluorozirconate (ZrF_4) glass was made in 1975.[5] ZrF_4 itself is not a glass but forms one when mixed with other fluorozirconate metals such as BaF_2 or SrF_2. In general, these glasses are not stable enough for use in bulk samples or fiber drawing and additional elements must be introduced. A common example of such a glass is ZBLAN. Fluorozirconate (or fluoride) glasses have many properties which make them ideal for low loss transmission in the 1550 nm region, e.g., a high transmission over a large range of wavelengths. For example, Rayleigh scattering in fluoride glasses has been predicted to be as low[6] as 0.003–0.007 dB/km and has been measured to be 0.025 dB/km at 2.25 μm.[7] These glasses also have much lower phonon energies compared to silica glasses and, thereby, a lower multiphonon edge.

In this paper, we report on solid glass microspherical resonators fabricated from a novel fluorozirconate, ZBNA ($ZrF_4-BaF_2-NaF-AlF_3$). ZBNA is a fluorozirconate ternary glass with 4 mol % of aluminum added for improved stability against devitrification, thereby making it more suitable for glass processing and bulk usage. It is also doped with 1.8 mol % of Er^{3+}. The interest in studying microspherical cavities arises from their potential use across a range of applications from the very applied areas of all-optical networks, biosensing, and miniature laser sources,[8] to fundamental experiments in which the microsphere can be used for investigating atom-photon interactions[9] and optical trapping of mesoscopic systems.[10] Such microcavities can be either active or passive depending on the material used and the application being studied. For example, we have previously shown[11] that certain emissions from Er^{3+} doped, ZBLALiP fluorozirconate glass microcavities are coincident with the resonance wavelengths of the D-2 transitions in cesium and rubidium - atoms that are routinely used in cold atom experiments. Optical bistability of stimulated emission lines[12] in Sm^{3+} doped glass microspheres was observed in 2001 and, subsequently, in Er^{3+}/Yb^{3+} codoped phosphate glass (IOG2) microcavities.[13] In the latter work, the effect is due to thermo-optical heating of the microsphere resulting in wavelength shifting of the microsphere's optical modes.

Here, the emission characteristics of Er^{3+} doped ZBNA microspheres are investigated and an ultralow green upconversion lasing threshold of ~3 μW is demonstrated. This is ten times lower than that previously reported for Er^{3+} doped ZBLAN pumped at 801 nm.[3] Thermo-optically induced bistability within the microsphere as a function of pump power is also explored and optical switching within the microcavity is demonstrated.

a)Electronic mail: jonathan.ward@tyndall.ie.
b)Electronic mail: S.NicChormaic@ucc.ie.

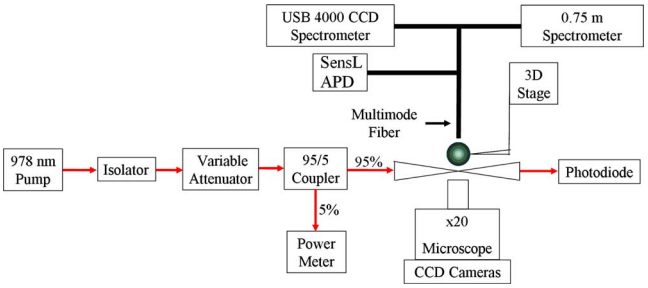

FIG. 1. (Color online) Schematic of experimental setup.

II. EXPERIMENT

Er^{3+} doped ZBNA microspheres with diameters ranging from 30 to 120 μm are used in the studies. The microspheres are fabricated from glass powder using a microwave plasma torch and the fabrication process has been described in detail elsewhere.[14] A schematic of the experimental setup used for acquiring the fluorescence and lasing is shown in Fig. 1. Pump light at 978 nm from a diode laser (Lasertron), with a laser linewidth of <0.065 nm, is coupled into and out of the microsphere via a tapered optical fiber with a diameter of 1 μm. The tapers are fabricated by heating and pulling single-mode fiber (Thorlabs, 1060XP) using an oxy-butane torch as the heat source. The transmission through the taper is typically better than 90% compared to the untapered fiber. Efficient coupling between the microsphere and taper is achieved by aligning the microsphere equator precisely with the taper via the use of piezocontrolled, precision translation stages. The 978 nm pump power is controlled using an electronic variable optical attenuator, thereby enabling a study of the fluorescence and lasing characteristics of the microsphere as a function of pump power. A 95:5 coupler is used to split the pump beam into a 5% channel for monitoring purposes, and a 95% channel used as the source of whispering gallery mode (WGM) excitation in the microsphere. Radiation within the microsphere can be evanescently coupled out into the exciting tapered fiber. However, the poor coupling efficiency of the visible fluorescence with the single-mode tapered fiber and the small signal-to-noise ratio of the 550 nm emissions to the 978 nm pump means that the transmitted visible fluorescence emission is difficult to detect from the end of the tapered fiber.[15] Alternatively, a multimode fiber connected to a *CCD* spectrometer (Ocean Optics USB 4000) can be used to measure the microsphere's visible fluorescence emission in free space. A fine spectrum of the green emissions can be acquired from a Princeton 0.75 m spectrometer (SpectraPro 2750) with a Pixis100 camera. Light from the microsphere is also collected using a microscope with up to 100× objective. Note that the Pixis camera can also be used to record the microscope image at low intensities.

III. RESULTS AND DISCUSSION

The absorption spectrum and phonon energy of ZBNA are nearly identical to those for Er^{3+} doped ZBLAN[16] and Er^{3+} doped ZBLALiP.[11] The low phonon energy[17] (<500 cm^{-1}) of ZBLAN and ZBNA ensures a long lifetime

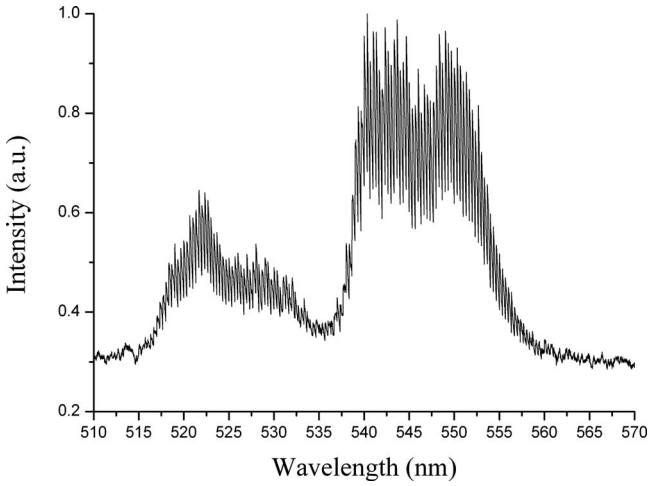

FIG. 2. Fine spectrum of the green emissions from a 60 μm ZBNA microsphere. An estimate of the sphere's Q-factor can be obtained by measuring the width of the fine peaks.

(>8 ms) of the intermediate $^4I_{11/2}$ state in the erbium energy levels.[11] The branching ratio of the $^4I_{11/2} \rightarrow {}^4I_{13/2}$ transition in Er^{3+} is from 10% to 20%.[11,18] The long lifetime and low branching ratio give a high upconversion rate, especially when pumped around 980 nm, making it difficult to efficiently populate the $^4I_{13/2}$ state which is responsible for emissions around 1550 nm.[18] For this reason, there are no fluorozirconate fiber amplifiers pumped around 980 nm. However, doping fluorozirconate glass with Ce ions (for example) can improve the branching ratio of the $^4I_{11/2} \rightarrow {}^4I_{13/2}$ transition by over 75%, thus achieving population of the metastable $^4I_{13/2}$ state.[18] By pumping Er^{3+} doped ZBNA at 978 nm one can study optical effects in the visible spectrum due to the very efficient upconversion process. During the experiments reported here, emissions between 1400 and 1600 nm for the Er^{3+} doped ZNBA microspheres were never observed. Recently, lasing emission around 1550 nm from a microsphere fabricated using a different Er^{3+} doped fluorozirconate glass (ZBLALiP) was demonstrated.[11] However, the lasing in ZBLALiP was generally weak, at typically less than a few nanowatt. It is believed that the higher phonon energy (~ 650 cm^{-1}) of ZBLALiP glass increases the phonon emission rate, therefore making the $^4I_{11/2} \rightarrow {}^4I_{13/2}$ transition more probable.

The results presented are mainly from three microspheres with diameters of 60, 65, and 75 μm. Emission bands at 470, 492, 520, 550, 656, 667, 793, and 849 nm have been observed from the Er^{3+} doped ZBNA microspheres. The intensity of the green emissions at 520 and 550 nm can be 60 and 30 times, respectively, greater than the others. A high resolution spectrum of the green upconversion fluorescence of a 60 μm sphere is shown in Fig. 2 with 1.5 s of integration.

Figure 3 shows the intensity of the 550 nm radiation as a function of the estimated absorbed pump power for the same 60 μm diameter sphere as used for Fig. 2. The green emissions were collected using a 20× microscope objective and detected using the Pixis camera in imaging mode. We focus on the 550 nm peak by using a band-pass filter with a 1 nm

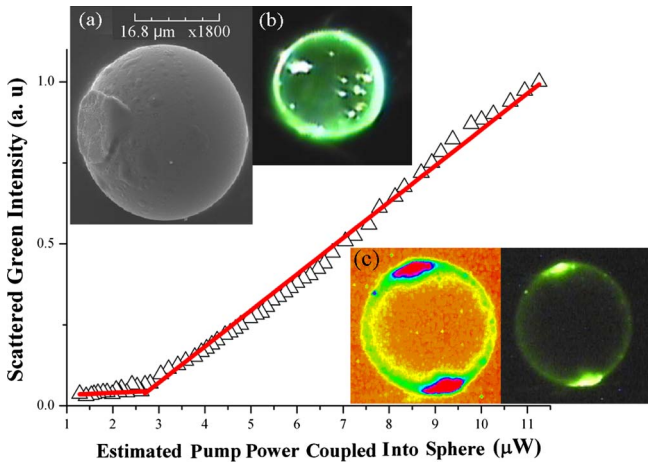

FIG. 3. (Color online) Intensity of the 550 nm output vs estimated pump power coupled into the microsphere. The solid line is a linear fit. Inset (a): SEM image of a ZBNA microsphere. Inset (b): optical image of 90 μm ZBNA microsphere showing multiple scattering points. Inset (c): optical image of a 60 μm ZBNA microsphere (right) and corresponding intensity map of the image (left), showing the WGM ring around the sphere's circumference. The two large bright points are due to scattering from internal or surface defects

bandwidth. The integration time of the camera was set to 2 s. One can see that the lasing threshold is ~3 μW, based on the estimated pump power coupled into the microsphere when 17 μW of pump power is launched into the tapered fiber at lasing threshold. This is the lowest threshold observed but could, in principle, be much lower since it strongly depends on the Q-factor of the sphere, the coupling efficiency, and the loss in the taper. The Q-factor was determined to be $\sim 10^3$ for the spheres in this work, estimated from the *FWHM* of one of the modes around 550 nm in the fine spectrum of the green emission in Fig. 2. The pump power coupled into the microsphere was estimated by multiplying the launched power into the fiber by the taper transmission and the change in transmission when the microsphere is in contact with the taper. The circulating intensity of the pump in the microsphere can be estimated from[19] $I = P_{\text{in}}(\lambda/2\pi n)(Q/V)$, where P_{in} is the input power, n is the group index, and V is the mode volume. The circulating intensity of the pump at lasing threshold is determined to be over 0.2 MW/m^2.

A scanning electron microscopy (SEM) image of a ZBNA microsphere is shown in inset (a) of Fig. 3. The image shows the surface to be coated by a flaky layer, believed to be the result of devitrification. Optical images of 90 and 60 μm ZBNA microspheres under pumping at 978 nm using a tapered optical fiber are shown in insets (b) and (c) of Fig. 3. The spheres are viewed from above and show the large number of scattering points in and around the mode path. Despite the poor quality of the microspheres, very low lasing thresholds were still observed.

In earlier work,[13] optical bistability over multiple wavelengths in an IOG2 phosphate glass microsphere was demonstrated and attributed to a thermo-optical effect. Phonon transitions excited after optical pumping around 978 nm generate heat in the glass. The subsequent rise in temperature causes a change in the refractive index of the glass and the size of the sphere, leading to a shift in the wavelength of the microsphere's optical modes. Boltzmann statistics can be used to describe the strong thermal coupling and the population redistribution between the two green levels in erbium, i.e., $^2H_{11/2}$ and $^4S_{3/2}$, and the intensity ratio of these two levels is a function of the internal cavity temperature.[20] Using this method, the mode volume temperature in some ZBNA microspheres was measured to be as high as 566 K, i.e., above the glass transition temperature of 538 K.[21] The thermal drift of the microsphere modes and thermal feedback near a pump/cavity resonance can result in bistable behavior.

The bistable operation in an undoped silica microsphere is described in detail by Mazumder *et al.*[22] and the effect is demonstrated experimentally in an undoped silica sphere by Carmon *et al.*,[23] where a narrow (relative to the cavity) linewidth pump laser is used. When the pump laser is initially tuned to the short wavelength side of a microsphere cavity mode and is then scanned toward the cavity mode, the approaching resonance condition causes heating of the microsphere that is maximal at zero pump/cavity resonance detuning. The increase in temperature shifts the cavity modes to longer wavelengths, and in this case,[23] away from the pump wavelength (so the wavelength of the pump mode is "chasing" the wavelength of the microsphere cavity mode). However, if the pump laser is initially tuned to the longer wavelength side of a microsphere cavity mode and is then scanned toward the cavity mode, the approaching resonance condition again heats the microsphere causing the cavity modes to shift to longer wavelengths but this time toward the pump wavelength (so the wavelength of the pump mode and the wavelength of the cavity mode are accelerated toward each other). This produces a hysteretic behavior to the intensity of transmitted pump power and the internal energy of the microsphere as a function of pump/cavity resonance detuning. The temperature increase observed by Carmon *et al.*[23] for a cavity resonant pump wavelength was relatively small (~6 K) due to the low material absorption of undoped silica at 1550 nm (or at 978 nm, for example) and the low power (<1 mW) launched into the taper.

For Er^{3+} doped glass microspheres pumped with a standard 978 nm diode laser (typically used in fiber amplifiers), the high material absorption from the Er^{3+} ions generates the heat and this can be significant even when the pump and microsphere cavity modes are nonresonant. In the following experiments, the 978 nm pump power launched into a 65 μm Er^{3+} doped ZBNA sphere via a tapered optical fiber was increased then decreased while the transmitted pump power was recorded. At the same time, the scattered 978 nm pump power was collected in free space using a multimode fiber [see Fig. 4(a)]. The maximum pump power launched into the tapered fiber is around 50 mW and the curve in the launched pump power is due to the nonlinear response of the electronic variable attenuator used, which was set to modulate between zero and full power. Heating the microsphere by increasing the pump power shifts the microsphere cavity modes to longer wavelengths. As a cavity mode approaches zero detuning from the stationary (in wavelength) pump mode, thermal feedback accelerates the shift rate of the cavity mode, quickly pushing the wavelength of the cavity mode

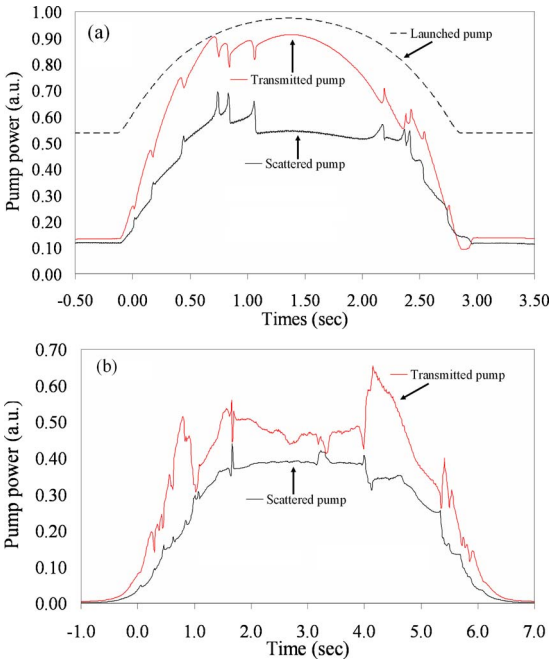

FIG. 4. (Color online) (a) Launched, scattered and transmitted pump power from a 65 μm sphere plotted as a function of time. The launched pump power has a curved shape due to the response of the electronic variable attenuator. As the launched pump power increases, pump/cavity resonant dips appear in the transmitted pump power, When the pump power is decreasing the same resonant dips appear again but at different pump powers and with a broadened line shape. The maximum launched pump power was ~50 mW and the maximum temperature recorded was 440 K. (b) Launched, scattered, and transmitted pump power from a 75 μm sphere plotted as a function of time. The maximum temperature recorded was 566 K giving an estimated mode shift of 2.2 nm.

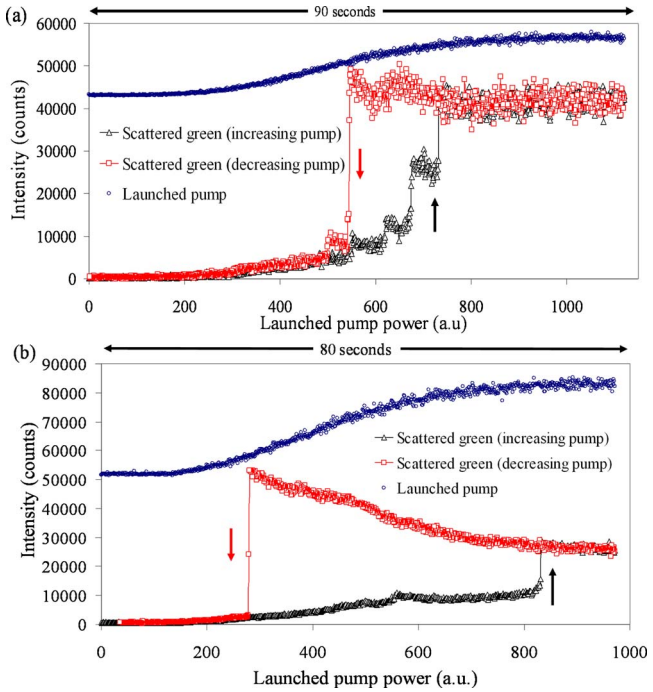

FIG. 5. (Color online) (a) Launched pump power and scattered green emission from a 75 μm sphere as a function of time. The multiple jumps in the green intensity correspond to multiple, coincidental pump/cavity resonances. (b) Launched pump power and scattered green emission from a 60 μm sphere as a function of time. Only a single pump/cavity resonance was encountered over the whole pump power range. The maximum pump power launched into the tapered fiber, in both cases, was 50 mW.

from the short wavelength side of the pump mode to the long wavelength side. For increasing pump powers, the resonances appear as narrow dips in the transmitted pump power. The higher the pump power on resonance, the faster the cavity mode will shift and the narrower the resonant dip in the transmitted power will appear. There is also an inherent distortion of the resonant line shape.[22–24]

Cooling the microsphere by reducing the pump power decreases the diameter of the microsphere and the sphere's modes are shifted to shorter wavelengths, back toward zero resonance detuning from the stationary pump mode. As the microsphere cools and the microsphere cavity mode moves back toward zero pump/cavity resonance detuning, the approaching resonance condition tries to heat the microsphere. The two opposing effects cause the microsphere cavity temperature to decrease at a slower rate and, as a result, the resonance dips in the transmitted power appear broadened for decreasing pump power, as shown in Fig. 4(a). In effect, the cavity mode looks like it is chasing the pump mode. This hysteresis in the microsphere's thermal shift rate causes the resonance dips in the transmitted power to occur at two different pump powers [see Fig. 4(a)] and produces different shapes to the resonant dips in the transmitted power.

The scan rate of a ZBNA microsphere mode can be determined from temperature measurements made during experiments. The maximum temperature increase recorded for the sphere used in Fig. 4(a) was $\Delta T = 140$ K. The thermal shift in the microsphere modes can be estimated from[20] $\Delta\lambda = \lambda \times \alpha \times \Delta T$, where the thermal expansion coefficient[20] $\alpha = 78 \times 10^{-7}/\mathrm{K}$ and this yields a total shift of 1.1 nm at 978 nm. The shift rate of the cavity resonance is assumed to be around 0.008 nm/K at 978 nm but the nm/mW value is dependent on how far detuned the cavity mode is from the pump mode. We have observed temperatures as high as 566 K in Er^{3+} doped ZBNA microspheres and, typically, the temperature increases sharply (by up to 50 K) when a coincidental pump/cavity resonance is encountered. This increase in temperature on resonance depends on the amount of pump power launched into the pump mode at that time.

Figure 4(b) shows the transmitted and scattered pump power from a 75 μm ZBNA microsphere where the maximum temperature recorded was 566 K. The wavelength shift for increasing pump power in Fig. 4(b) is estimated to be around 2 nm. The higher temperature means a larger shift in the microsphere modes and, therefore, a higher probability that more pump/cavity resonances are observed.

In a separate experiment the launched pump power is increased then decreased while the green emission scattered from a 75 μm ZBNA microsphere is collected using a multimode fiber. The collected light is sent to a SensL dual-channel avalanche photodiode[25] and photon counting module, see Fig. 5, and the scattered pump power was filtered out in order to improve the signal-to-noise ratio. The multiple intensity jumps in the scattered green intensity, for increasing pump power shown in Fig. 5(a), corresponds to multiple coincidental pump/cavity resonances. When the pump power is decreased, the bistable operation becomes clearly visible. The intensity of all the upconversion channels closely fol-

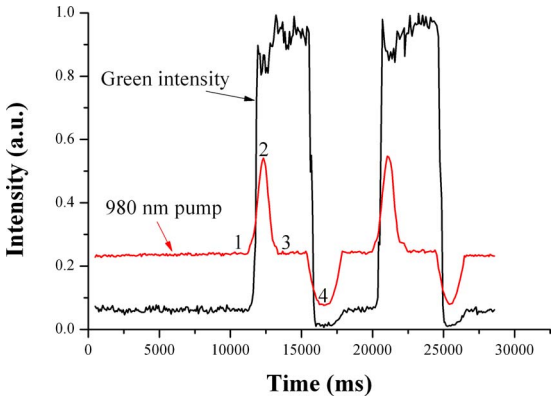

FIG. 6. (Color online) Scattered green emission (black curve) and pump power (red curve) vs time. Points 1–4 indicate the switching states for the fluorescence.

lows this bistable operation. Figure 5(b) shows the scattered green emission as a microsphere mode is thermally shifted across a single pump/cavity resonance. Here, there was only one pump/cavity resonance over the entire pump power range; the temperature increase on resonance is ~50 K. Sometimes it is possible to go from a single intensity jump to multiple jumps just by changing the position of the tapered optical fiber relative to the microsphere and/or the wavelength of the pump. The green emission has the largest contrast ratio (i.e., the ratio between the low output and the high output) and, in some microspheres, this can be as high as 125.

Finally, in a separate experiment, the latching behavior of the bistable switch was investigated and is illustrated in Fig. 6. The pump intensity is initially at point 1 and is then briefly increased to point 2. At point 3 in Fig. 6, the pump is the same as at point 1. However, the green fluorescence intensity at point 3 is 15 times higher than at point 1. The green intensity remains high until the pump is reduced at point 4 and this resets the latch. The frequency of the pump signal is 0.11 Hz and is limited by the speed of the variable attenuator. The maximum speed of such a switch would be limited by the thermal properties of the glass and/or the lifetime of the erbium energy level involved, which for the 550 nm $^2H_{11/2} \rightarrow {}^4I_{15/2}$ transition is ~0.9 ms.

IV. CONCLUSION

In conclusion, green lasing and optical bistability from Er^{3+} doped ZBNA microspheres fabricated using a microwave plasma torch and pumped at 978 nm have been demonstrated. SEM and optical images indicate that the quality of the spheres is relatively poor. However, the measured lasing threshold is exceedingly low at 3 μW, ten times lower than that obtained for Er^{3+} doped ZBLAN microspheres. So far, this is the lowest threshold value observed and the average threshold is around 10 μW. We observed no indication of saturation of the green emission for a maximum of 50 mW launched into the tapered fiber.

Optical bistability within the Er^{3+} doped ZNBA microspheres has also been observed. The bistability occurs in the emission intensity and in the wavelength of the microsphere's optical modes as a function of launched pump power. In this case, i.e., for doped microspheres and a constant pump wavelength, the apparent broadening of the resonance is observed as the cavity is being shifted toward shorter wavelength, in contrast to that reported by Carmon *et al.*,[23] where the apparent broadening occurs as the cavity mode is shifted toward longer wavelengths. This is because the wavelength of the microspheres modes and the pump power are being scanned, as opposed to the pump wavelength.

Doped microsphere lasers are most efficient when the pump laser is tuned to a pump/cavity resonance. However, if the pump is tuned to the short wavelength side of the resonance the microsphere laser emission can become unstable due to positive thermal feedback, i.e., small changes in cavity temperature are amplified. In contrast, if the pump is tuned to the long wavelength side of a pump/cavity resonance, then the laser emission can have some degree of self-stabilization due to negative thermal feedback, i.e., small changes in cavity temperature are damped. From this, self-stabilization against small changes in pump power or temperature could possibly be achieved if the cavity is detuned to the long wavelength side of the pump/cavity resonance. Multiple bistable loops, corresponding to multiple coincidental pump/cavity resonances, have also been demonstrated.

A separate experiment illustrating the latching behavior of the microspheres shows that these devices could be suitable as low frequency, all-optical latches. Currently the setup is limited by the speed and response of the variable attenuator. With the addition of an acousto-optical modulator it should be possible to measure the switching speed of the microsphere and the lifetimes of the Er^{3+} energy levels.

ACKNOWLEDGMENTS

This work was funded by Science Foundation Ireland under Grant Nos. 02/IN1/128 and 07/RFP/PHYF518s2. Y.W. acknowledges support from IRCSET through the Embark Initiative. The authors wish to acknowledge generous assistance from P. Féron, ENSSAT, Lannion, France for providing the ZBNA microspheres.

[1] T. J. Whitley, C. A. Millar, R. Wyatt, M. C. Brierley, and D. Szebesta, Electron. Lett. **27**, 1785 (1991).
[2] H. Fujiwara and K. Sasaki, J. Appl. Phys. **86**, 2385 (1999).
[3] W. von Klitzing, E. Jahier, R. Long, F. Lissillour, V. Lefèvre-Seguin, J. Hare, J. M. Raimond, and S. Haroche, J. Opt. B: Quantum Semiclassical Opt. **2**, 204 (2000).
[4] T. Lu, L. Yang, R. V. A. van Loon, A. Polman, and K. J. Vahala, Opt. Lett. **34**, 482 (2009).
[5] M. Poulain, J. Lucas, and P. Brun, Mater. Res. Bull. **10**, 243 (1975).
[6] M. E. Lines, J. Appl. Phys. **55**, 4058 (1984).
[7] L. E. Busse, G. H. McCabe, and I. D. Aggarwal, Opt. Lett. **15**, 423 (1990).
[8] J. M. Ward, P. Féron, and S. Nic Chormaic, IEEE Photonics Technol. Lett. **20**, 392 (2008).
[9] F. Treussart, J. Hare, L. Collot, V. Lefèvre, D. S. Weiss, V. Sandoghdar, J. M. Raimond, and S. Haroche, Opt. Lett. **19**, 1651 (1994).
[10] J. M. Ward, Y. Wu, V. G. Minogin, and S. Nic Chormaic, Phys. Rev. A **79**, 053839 (2009).
[11] D. G. O'Shea, J. M. Ward, B. J. Shortt, M. Mortier, P. Féron, and S. Nic Chormaic, Eur. Phys. J.: Appl. Phys. **40**, 181 (2007).
[12] T. Hayakawa, H. Ooishi, and M. Nogami, Opt. Lett. **26**, 84 (2001).
[13] J. M. Ward, D. G. O'Shea, B. J. Shortt, and S. Nic Chormaic, J. Appl. Phys. **102**, 023104 (2007).

[14]F. Lissillour, K. Ait Ameur, N. Dubreuil, G. M. Stephan, and M. Poulain, Proc. SPIE **3416**, 150 (1998).
[15]K. Bondarczuk, P. J. Maguire, L. P. Barry, J. O'Dowd, W. H. Guo, M. Lynch, A. L. Bradley, J. F. Donegan, and H. Folliot, IEEE Photonics Technol. Lett. **19**, 21 (2007).
[16]C. Wanghe, K. Shidong, and Z. Chuanyi, Proc. SPIE **3557**, 27 (1998).
[17]R. S. Deol, D. W. Hewak, S. Jordery, A. Jha, M. Poulain, M. D. Baró, and D. N. Payne, J. Non-Cryst. Solids **161**, 257 (1993).
[18]Z. Meng, J. Kamebayashi, M. Higashihata, Y. Nakata, T. Okada, Y. Kubota, N. Nishimura, and T. Teshima, IEEE Photonics Technol. Lett. **14**, 609 (2002).
[19]K. J. Vahala, Nature (London) **424**, 839 (2003).
[20]P. Féron, C. Arnaud, M. Boustimi, G. Nunzi-Conti, G. Righini, and M. Mortier, Proc. SPIE **5451**, 199 (2004).
[21]O. Péron, B. Boulard, Y. Jestin, M. Ferrari, C. Duverger-Arfuso, S. Kodjikian, and Y. Gao, J. Non-Cryst. Solids **354**, 3586 (2008).
[22]M. M. Mazumder, S. C. Hill, D. Q. Chowdhury, and R. K. Chang, J. Opt. Soc. Am. B **12**, 297 (1995).
[23]T. Carmon, L. Yang, and K. Vahala, Opt. Express **12**, 4742 (2004).
[24]C. Schmidt, A. Chipouline, T. Pertsch, A. Tünnermann, O. Egorov, F. Lederer, and L. Deych, Opt. Express **16**, 6285 (2008).
[25]www.sensl.com